

COMPUTATIONAL MODELLING OF THE RIGHT VENTRICLE IN REPAIRED TETRALOGY OF FALLOT: CAN IT PROVIDE INSIGHT INTO PATIENT TREATMENT?

B. Leonardi¹, A.M. Taylor², T. Mansi³, I. Voigt^{3,4}, M. Sermesant⁵, X. Pennec⁵, N. Ayache⁵, Y. Boudjemline⁶, G. Pongiglione¹.

¹Bambino Gesù Children's Hospital and Research Institute, Rome, Italy

²UCL Institute of Cardiovascular Sciences & Great Ormond Street Hospital for Children, London, UK

³Siemens Corporation, Corporate Research and Technology, Imaging and Computer Vision, Princeton, NJ, USA

⁴Friedrich-Alexander-University, Pattern Recognition Lab, Erlangen, Germany

⁵Asclepios Research Team, INRIA Sophia Antipolis, France

⁶Université Paris Descartes, Assistance Publique des Hopitaux de Paris, Necker Hospital for Sick Children, Paris, France

Part of the FP6 Health-e-Child (HeC) project (European project, IST-2004-027749)
Relationship with Industry (Siemens was the industrial partner in the Health-e-Child project)

Correspondence to:

Professor Andrew Taylor, MD, FRCP, FRCR

UCL Institute of Cardiovascular Science & Great Ormond Street Hospital for Children

Great Ormond Street Hospital for Children

Great Ormond Street

London, WC1N 3JH

United Kingdom

Email: a.taylor76@ucl.ac.uk

Telephone: +44 20 7405 9200 (ext. 5616)

Total word count (entire document): 4551

Abstract word count: 248

Keywords: 4

Tables: 2; Figures: 3

Abstract

Aims: Pulmonary regurgitation (PR) causes progressive right ventricle (RV) dilatation and dysfunction in repaired tetralogy of Fallot (rToF). Declining RV function is often insidious and the timing of pulmonary valve replacement remains under debate. Quantifying the pathophysiology of adverse RV remodelling due to worsening PR may help in defining the best timing for PVR. Our aim was to identify whether complex three-dimensional (3D) deformations of RV shape, as assessed with computer modelling, could constitute an anatomical biomarker that correlated with clinical parameters in rToF patients.

Methods and Results: We selected 38 rToF patients (aged 10-30 years) who had complete datasets and had not undergone PVR from a population of 314 consecutive patients recruited in a collaborative study of four hospitals. All patients underwent cardiovascular magnetic resonance (CMR) imaging: PR and RV end-diastolic volumes were measured. An unbiased shape analysis framework was used with principal component analysis and linear regression to correlate shape with indexed PR volume. Regurgitation severity was significantly associated with RV dilatation ($p=0.01$) and associated with bulging of the outflow tract ($p=0.07$) and a dilatation of the apex ($p=0.08$).

Conclusion: In this study, we related RV shape at end diastole to clinical metrics of PR in rToF patients. By considering the entire 3D shape, we identified a link between PR and RV dilatation, outflow tract bulging and apical dilatation. Our study constitutes a first attempt to correlate 3D RV shape with clinical metrics in rToF, opening new ways to better quantify 3D RV change in rToF.

Keywords: Computer modelling, right ventricle, tetralogy of Fallot, pulmonary regurgitation

Introduction

Early surgical repair of tetralogy of Fallot often leaves patients with residual pulmonary regurgitation (PR), which is associated with significant late complications – exercise intolerance, right heart failure, arrhythmias and sudden death.¹⁻³ Pulmonary valve replacement (PVR)^{4,5} in repaired tetralogy of Fallot (rToF) has become the treatment of choice to treat late PR, and halt or at least slow down the progression of adverse right ventricular (RV) remodelling and its sequelae. Unfortunately, PVR is not a definitive therapeutic option and clinicians have to balance the immediate benefits of PVR against the likelihood of long-term complications and the need for future re-intervention. Accurate follow-up of patients is necessary, often with serial assessment of RV size and systolic function, using cardiovascular magnetic resonance (CMR) imaging;⁶⁻¹⁰ however, there are no clear, evidence-based guidelines on the optimal timing for PVR.¹¹

Computational modelling analysis of congenital heart disease,¹² and in particular how RV dilatation evolves over time, could provide insights into pathological mechanisms, resulting in a useful support tool for disease evaluation and therapy planning. RV and RV outflow tract anatomy are complex and vary significantly among rToF patients^{13,14} and therefore quantifying the entire RV shape is challenging. Recently, we have described a new method of computational modelling to analyze 3D shapes and compare them with clinical features for the RV.¹⁵ A few studies have partially analyzed the 3D alterations of the RV anatomy in rToF.^{16,17} Results from these studies suggest important differences in regional RV remodelling, but could not identify local changes in RV anatomy because the volume metrics used were too coarse.

In the present study, our aim was to investigate the clinical applicability of our computational modelling method. Assuming that RV shape can provide insight into the heart condition, we applied our shape analysis method to establish new quantitative metrics based on the RV shape that may assist in helping to plan when individual patients should undergo PVR. In particular, we aimed at identifying abnormal RV shape features that could reveal severe deterioration in the cardiac structure due to PR, which together with the clinical parameters may help in timing of PVR.

Methods

Subjects

As part of a collaborative study involving four hospitals (Gaslini Institute, Genoa, Italy; Great Ormond Street Hospital for Children, London, U.K.; Hôpital Necker – Enfants Malades, Paris, France; Bambino Gesù Children's Hospital and Research Institute, Rome, Italy;) every willing, consecutive patient with rToF was recruited over a 3-year period (n=314), as part of the FP6 Health-e-Child project (European project, IST-2004-027749). Local ethical approval was given by all four hospitals for the research, and informed consent was received from the patients (and/or their legal guardians) to partake in the study.

From the 314 patients enrolled into the Health-e-Child project, 49 had complete datasets that enabled them to be included in our current study (clinical features, echocardiogram, full CMR examination and right ventricle segmentation). These datasets were used to define a representative RV shape for the group. Subsequent analysis of shape and pulmonary regurgitation volume was carried out on the 38 patients (26 males), from these 49 who had not undergone PVR prior to CMR. The majority of these patients (n=35) had had transannular surgery at their initial repair. Clinical features of these patients are reported in Table 1. Figure 1 summarizes the different steps of our analysis.

Imaging assessment

CMR exams were acquired with 1.5T MR scanners (Avanto, Siemens and Achieva, Philips). The standard approach to measure RV volume and function using cine imaging (balanced steady-state free precession sequences), with multiple short-axis

slices covering entirely both ventricles acquired during breath-holding (10-15 slices; in-plane resolution: 1.1 to 1.7 mm²; slice thickness: 5 to 8 mm; 25 to 40 phases). Manual tracking of the endocardial contours allowed the measurement of EDV, ESV, stroke volume (SV) and RV ejection fraction (EF). Flow quantification was performed using through-plane phase contrast velocity mapping, with a retrospectively gated, gradient echo sequence, during free respiration technique (slice thickness 8 mm, TE 2.7 ms, TR 4.7 ms, acquisition matrix 176 x 512). Pulmonary regurgitant fraction (PRF) was calculated as pulmonary retrograde flow (mL/beat) x 100/pulmonary forward flow (mL/beat). Then pulmonary regurgitant volume (PRV) was indexed for BSA to give PRVi.

Surface Mesh Preparation

We studied the RV shape at end-diastole, when the anatomical features of the pathology are more pronounced.¹⁶ The RV endocardium was segmented on the end-diastolic CMR cine images by fitting an anatomically accurate geometrical model.¹⁸ In brief, RV position, orientation, scale and boundaries in the images were determined automatically using machine-learning algorithms based on marginal space learning and probabilistic boosting tree. An expert manually adjusted the automatic fitting whenever it was necessary (Figure 2, left panel). At the end of the process, 3D meshes of the RV were available for every patient (Figure 2, mid-panel). In the subsequent text, we refer to these meshes as shapes. To avoid any bias in the statistical analyses due to patient positioning, the 3D meshes were rigidly aligned in a common coordinate system using a standard least-square method.¹⁹

RV Shape Representation and Quantification

Right ventricles were investigated by analyzing how an ideal reference shape – the template (developed from the 49 patients) – deforms in a population of shapes – here the set of RV meshes computed from the CMR data of our patients. Intuitively, if the template is deformed in such a way that it matches the RV shape of a patient, then the deformation that is applied encodes the shape information of that patient. A rigorous mathematical framework can then be employed on the non-linear deformations to analyze the shapes.²⁰ Although any RV shape can be taken as the reference, to avoid any bias in the analysis, it is highly recommended to use a template that is as independent as possible from the studied population and that is ‘centred’ – i.e. equally distant to all subjects. In this study, we estimated the template using the method proposed by Durrleman et al.²⁰ Indeed, we have demonstrated in our previous study¹⁵ that the resulting template is robust with respect to rToF subjects and is well centred, thus constituting a suitable reference. Our computer modelling process is as follows: We start from a template (the mean shape, represented by mathematical currents – see^{20,21}). We then compute the transformations that deform this template to the RV shapes of our patients.²¹ Using these transformations, we update the template such that it minimizes the residual errors of the template-to-patient matching. We repeat these two steps iteratively until convergence. At the end of the process, we obtain an unbiased template of the RV and the related deformations. It can be observed that in such a framework, the template and the deformations are calculated simultaneously, a key requirement for a consistent shape analysis (see^{15,20,21} for mathematical details). It should be stressed that the computed template is an ideal geometry representing the average RV observed in the population. As such, no clinical data is available for this template. In

particular, this ideal RV does not come from any individual patient's CMR data, but rather represents the entire population under study.

Compact Representation of Patient RV Shape

The non-linear deformations computed in the previous step, which encode patient RV shapes, make it possible to quantitatively correlate RV shape with clinical variables. However, direct statistics on these deformations was not possible as they were represented by too many parameters (>1000) to have a good statistical power. To reduce the dimensionality of the problem, we thus performed a principal component analysis (PCA) of the deformations (see^{15,20}). The 38 patients under study were used to compute the principal components of the deformations. The PCA modes, called deformation modes, represented a specific pattern of RV shape variation observed in this population (e.g. overall dilatation, apical bulging, etc.). Since this pattern is computed from the entire population, it is not related to specific clinical data or CMR images. By projecting patient deformations into the PCA space, we could represent each patient by a low-dimensional shape vector whose elements quantified the contribution of each deformation mode in patient RV shape. In other words, by definition of the PCA, the RV shape of a given patient is the weighted sum of all computed deformation modes, the weights varying from patient to patient. As the number of elements of the shape vector was lower than the number of patients, standard statistical designs could be applied to quantitatively correlate the RV features identified by the PCA modes with clinical features.

Identification of Pathological Shape Features

To identify shape features related to regurgitation, we related the shape vectors to indexed PR volume (PRVi) using linear regression with automatic model reduction according to Akaike Information Criterion. We used indexed measurements to remove growth effects from the analysis. The idea was to estimate a reduced linear model that predicted the PRVi (measured variable) from the elements of the shape vectors (predictors). The deformation modes corresponding to the elements selected in the model encoded the 3D shape features that were related to PRVi, which we could visualize and quantify by deforming the reference template with these deformation modes. The sign of the linear regression coefficients identified the direction of correlation along the deformation mode for increasing PRVi. All the tests were performed with R (R Development Core Team, 2009). The level of significance was set at $p < 0.05$.

Results

Template of the Right Ventricle

Figure 2, left-panel shows a 3D RV mesh overlaid on the CMR image of a patient. Figure 2, mid-panel illustrates the RV meshes of all patients aligned in a common coordinate system. Since the overall study was retrospective, only 49 patients out of 314 had complete CMR data. To avoid any bias we thus computed the template using all available patients. Figure 2, right panel illustrates the RV template estimated from the 49 patients. The template was well centred with respect to the population, as quantified by the standardized mean of deformations, $mean/sd = 0.4 < 1$. Interestingly, the patient's age that was closest to the template was 16 years whose BSA was 1.64 m^2 . Both values were close to population average (Table 1), which suggests a good consistency between the template and the above-mentioned clinical features.

Relating the Right Ventricle Shape to Pulmonary Regurgitation

Twenty deformation modes encoded 95% of shape variability observed in our population who had not undergone PVR ($n=38$), resulting in 20-element shape vectors. The optimal linear model consisted of six PCA modes (Table 2) ($R^2 = 0.39$, $p = 0.013$). Three deformation modes were found statistically relevant to the model. Mode 1 was significantly and positively related to increasing PRVi ($p=0.01$), whilst there was a positive association with Mode 12 ($p=0.07$) and a negative association with mode 15 ($p=0.08$). Applying these deformation modes onto the template enabled us to visualize and quantify the shape changes. From Figure 3, we observed that in our population, PRVi is related to RV global enlargement (mode 1), bulging of the outflow tract towards an aneurismal shape (mode 12 and 15), dilatation of the RV

apex (mode 12 and 15), dilatation of the pulmonary valve annulus and a more circular tricuspid valve. These findings are consistent with previous results on a different population.^{15,22}

Discussion

To the best of our knowledge, this study constitutes a first attempt to correlate 3D RV shape with clinical parameters in patients with rToF using computer modelling. We have shown in a realistic way that the RV dilates (the outlet bulges and the apex deforms) as pulmonary regurgitation volume worsens. Due to the fact that our approach considers the complete 3D shape on a regional level, it could constitute a useful tool for the management of rToF patients by providing quantitative features of RV shape that are more discriminating compared to standard CMR analysis, which relies only on the volume.

While our findings are relatively known and our work is similar to Sheehan et al., 2008,¹⁶ our approach is radically different and opens new avenues in the shape analysis of the cardiac chambers. While Sheehan et al. analyzed specific lumped markers from the 3D shape, we assess the entire 3D shape analyzed directly, without the introduction of any prior knowledge, which is implicitly the case when selecting specific metrics. As a result, we can now identify more subtle features that cannot be encoded by lumped metrics easily. The features related to PR are automatically extracted by the correlation analysis. It is therefore interesting to see that we can recover the main features of rToF using our approach.

Though RV volume is one of the outcome predictors in rToF patients, chamber geometry, myofiber architecture, RV compliance, chamber contraction pattern and the interdependence between LV and RV function are likely to play a role in defining the long-term outcomes for rToF patients. In addition, any RV outflow tract patch and the consequent localized fibrosis and akinesis/dyskinesis of the RV outflow tract,

which vary from patient to patient, may play a role in pathophysiology.²³ Assessment of the RV outflow tract remains difficult on both CMR and echo^{24,25} and an overall 3D assessment of RV shape may prove to be a useful biomarker. The methods we describe could give us a more realistic and complete view of 3D RV shape, which may give further insight into the timing of PVR, though larger scale studies to assess the usefulness of such a new biomarker would need to be performed. Importantly, though our method has been developed using CMR data, it could be applied to 3D echo data, to act as a surrogate for pulmonary regurgitation severity. As semi-automatic or fully automatic methods are available to segment the heart on echo images, the resulting meshes could then be directly used in our framework to extract shape features. Other functional parameters, such as Doppler flow metrics or strain could also be included in the statistical analysis for a more comprehensive correlation between shape and function.

Although there is strong evidence that PVR is safe and effective at eliminating or greatly reducing pulmonary regurgitation, it should be kept in mind that in the majority of studies global RV systolic function remains unchanged. Moreover, at present, data regarding the effects of PVR on arrhythmia propensity and objective exercise parameters are inconsistent. Therefore, having additional information may be useful for defining patient outcomes. In addition, our model can be useful to quantify the degree of bulging by computing the RV shape vector of a patient, an index that could be used as a predictor of PVR. Thus, it could be helpful not only to facilitate the decision on the right timing and type of surgical approach, but also to monitor the effect of chronic pulmonary regurgitation and, consequently, the volume load on RV mechanics during the life of a specific rToF patient.

In the future, we could perform analysis with BSA, patient age¹⁵, and gender²⁶ to understand how RV shape changes in relation to growth, and use such models to predict the pulmonary regurgitant volume over time. Deviation from what is known to be the 'normal', predicted RV shape change for any given individual patient might alert us to sub-clinical deterioration in RV function that could trigger closer clinical follow-up or even early PVR. Whilst patients who are doing better than expected may be able to have PVR deferred. Furthermore, analysis of the LV-RV interaction by directly applying our segmentation and shape methodology of the bi-ventricular myocardium could provide further novel information. Finally, our approach might also be applied on post-operative data to study the long-term impact of new PVR therapies on RV anatomy.^{27,28}

Limitations: A drawback of this study is the lack of control subjects that, unfortunately, prevented us from studying the differences between rToF patients and healthy subjects, as in the study of Zhang *et al.*²⁹ Furthermore, we have analysed a relatively small number of patients to estimate the template, as CMR data was not available retrospectively in all patients recruited for the Health-e-Child study. Future work should include the analysis of a larger population to confirm our findings.

Conclusions: We have provided new insights into the mechanical adaptation of RV to chronic significant pulmonary insufficiency in rToF patients. The measurement of an RV shape biomarker may allow for personalized follow-up of rToF patient, which may help defining the timing of PVR.

Acknowledgments: This work was funded as part of the FP6 EU project Health-e-Child. AMT is funded by the National Institute of Health Research and the Fondation Leducq. The authors sincerely thank Dr. Andreina Santoro for her kind revision of the manuscript.

Tables

Table 1: Clinical features of 38 rToF patients (mean \pm standard deviation).

38 patients with rToF	
Age	16.34 \pm 4.38 year
Body surface area	1.56 \pm 0.36 m ²
Pulmonary regurgitant fraction (PRF)	43.32 \pm 11.77 %
Indexed pulmonary regurgitant volume (PRVi)	31.79 \pm 15.73 mL/beat/m ²

Table 2: Regression coefficients between the shape vectors and PRVi after model reduction ($R^2 = 0.39$, $P = 0.013$). Six modes were kept. The sign of the coefficients indicates the direction of correlation for increasing PRVi. In bold the modes that were relevant to PRVi.

	Estimate	Std. Error	t-value	p-value
(Intercept)	34.7212651	2.2253078	15.603	3.14E-16
Mode1	0.0025349	0.0009366	2.706	0.011
Mode2	0.0045411	0.0034199	1.328	0.1939
Mode10	-0.0163286	0.0124469	-1.312	0.1992
Mode12	0.0264241	0.0142791	1.851	0.0738
Mode15	-0.0394336	0.0221589	-1.78	0.085
Mode18	-0.0410802	0.0272007	-1.51	0.1411

Figures

Figure 1: Analysis pipeline. The RV were first segmented from cardiac MRI. A reference template and the deformations, which mapped that template to each RV, were then computed to quantify RV shapes. PCA on deformations was performed to extract the main shape variation features and reduce model dimension. Linear regression was finally estimated to identify the shape features related to PRVi. See text for details.

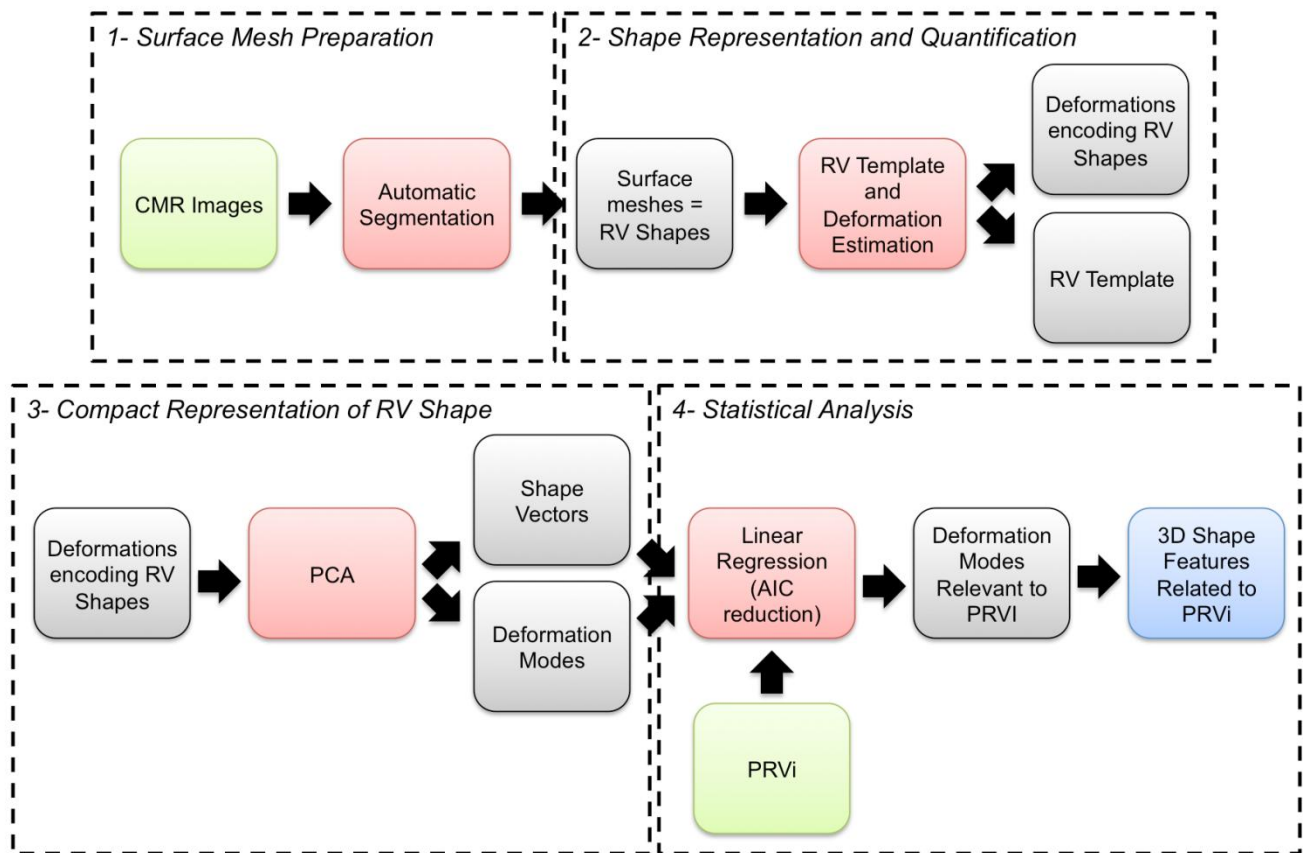


Figure 2: Left panel: 3D RV mesh of a patient overlaid on its CMR. Mid panel: 3D RV meshes of 49 patients segmented from CMR and rigidly aligned to a common coordinate frame. Observe the large variability in shape. Right panel: Mean RV shape of the population

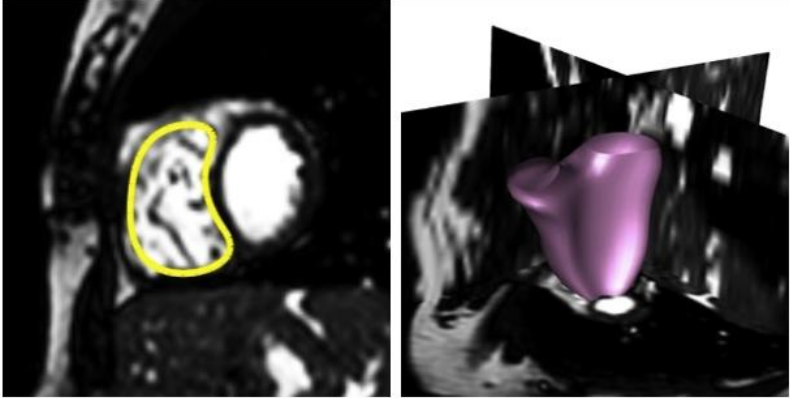
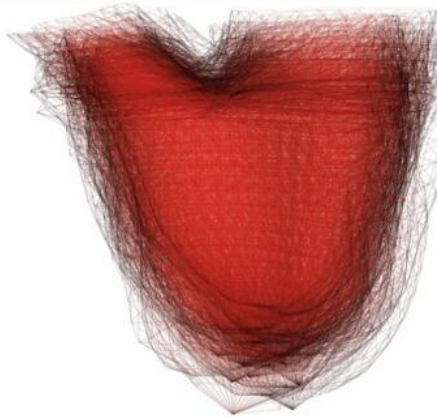
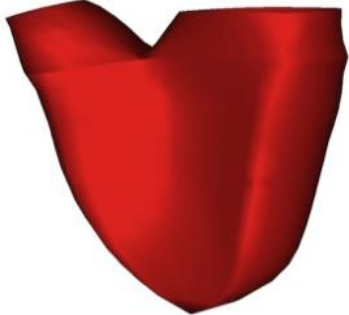
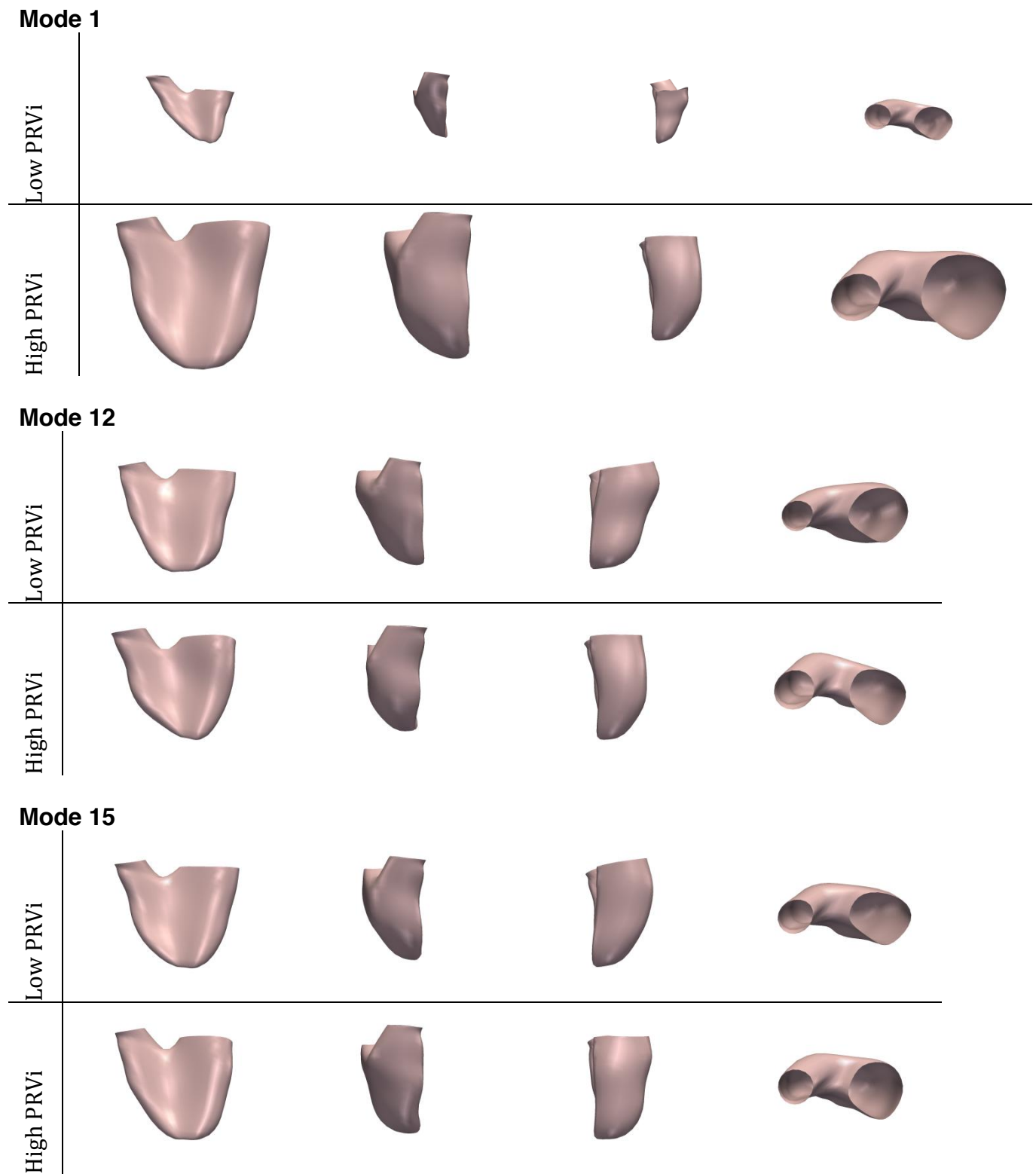
RV mesh overlaid on CMR Short-axis (left) and 3D (right) views	RV of 49 Patients Rigidly Aligned	Mean RV Shape
		

Figure 3: Variations in RV shape correlated with PRVi in 38 patients. Modes 1, 12 and 15 were found significantly related to PRVi.



References

- 1) Nollert G, Fischlein T, Bouterwek S, Böhmer C, Klinner W, Reichart B. Long-term survival in patients with repair of tetralogy of Fallot: 36-year follow-up of 490 survivors of the first year after surgical repair. *J Am Coll Cardiol* 1997; **30(5)**: 1374-83.
- 2) Gatzoulis MA, Balaji S, Webber SA, Siu SC, Hokanson JS, Poile C, Rosenthal M, Nakazawa M, Moller JH, Gillette PC, Webb GD, Redington AN. Risk factors for arrhythmia and sudden cardiac death late after repair of tetralogy of Fallot: a multicentre study. *Lancet* 2000; **356**: 975-81.
- 3) Geva T, Sandweiss BM, Gauvreau K, Lock JE, Powell AJ. Factors associated with impaired clinical status in long-term survivors of tetralogy of Fallot repair evaluated by magnetic resonance imaging. *J Am Coll Cardiol* 2004; **43(6)**:1068-74.
- 4) Dos L, Dadashev A, Tanous D, Ferreira-González IJ, Haberer K, Siu SC, Van Arsdell GS, Oechslin EN, Williams WG, Silversides CK. Pulmonary valve replacement in repaired tetralogy of Fallot: determinants of early postoperative adverse outcomes. *J Thorac Cardiovasc Surg* 2009; **138(3)**: 553-9.
- 5) Lurz P, Coats L, Khambadkone S, Nordmeyer J, Boudjemline Y, Schievano S, Muthurangu V, Lee TY, Parenzan G, Derrick G, Cullen S, Walker F, Tsang V, Deanfield J, Taylor AM, Bonhoeffer P. Percutaneous pulmonary valve implantation: impact of evolving technology and learning curve on clinical outcome. *Circulation* 2008; **117(15)**:1964-72.
- 6) Geva T. Repaired tetralogy of Fallot: the roles of cardiovascular magnetic resonance in evaluating pathophysiology and for pulmonary valve replacement decision support. *J Cardiovasc Magn Reson* 2011; **13**:9.

- 7) Therrien J, Provost Y, Merchant N, Williams W, Colman J, Webb G. Optimal timing for pulmonary valve replacement in adults after tetralogy of Fallot repair. *Am J Cardiol* 2005; **95(6)**: 779-82.
- 8) Buechel ER, et al. Remodelling of the right ventricle after early pulmonary valve replacement in children with repaired tetralogy of Fallot: assessment by cardiovascular magnetic resonance. *Eur Heart J* 2005; **26**:2721-7.
- 9) Oosterhof T, Meijboom FJ, Vliegen HW, Hazekamp MG, Zwinderman AH, Bouma BJ, van Dijk AP, Mulder BJ. Long-term follow-up of homograft function after pulmonary valve replacement in patients with tetralogy of Fallot. *Eur Heart J* 2006; **27(12)**: 1478-84.
- 10) Lee C, et al. Outcomes of Pulmonary Valve Replacement in 170 Patients With Chronic Pulmonary Regurgitation After Relief of Right Ventricular Outflow Tract Obstruction: Implications for Optimal Timing of Pulmonary Valve Replacement. *J Am Coll Cardiol* 2012; **Aug 15**. [Epub ahead of print] doi:10.1016/j.jacc.2012.03.077
- 11) Baumgartner H, et al. ESC Guidelines for the management of grown-up congenital heart disease (new version 2010). *Eur Heart J* 2010; **31**:2915-57.
- 12) Hsia TY, Cosentino D, Corsini C, Pennati G, Dubini G, Migliavacca F, Modeling of Congenital Hearts Alliance (MOCHA) Investigators. Use of mathematical modeling to compare and predict hemodynamic effects between hybrid and surgical Norwood palliations for hypoplastic left heart syndrome. *Circulation* 2011; **124(11 Suppl)**:S204-10.
- 13) Schievano S, Migliavacca F, Coats L, Khambadkone S, Carminati M, Wilson N, Deanfield JE, Bonhoeffer P, Taylor AM. Planning of percutaneous pulmonary valve implantation based on rapid prototyping of the right ventricular outflow tract and

- pulmonary trunk from magnetic resonance imaging data. *Radiology* 2007; **242(2)**: 490-497.
- 14) Schievano S, Coats L, Migliavacca F, Norman W, Frigiola A, Deanfield J, Bonhoeffer P, Taylor AM. Variations in Right Ventricular Outflow Tract Morphology following Repair of Congenital Heart Disease - Implications for Percutaneous Pulmonary Valve Implantation. *JCMR* 2007; **9(4)**:687-95.
 - 15) Mansi T, Voigt I, Leonardi B, Pennec X, Durrleman S, Sermesant M, Delingette H, Taylor AM, Boudjemline Y, Pongiglione G, Ayache N. A statistical model for quantification and prediction of cardiac remodeling: application to tetralogy of Fallot. *IEEE Trans Med Imaging* 2011; **30(9)**:1605-16.
 - 16) Sheehan FH, Ge S, Vick GW 3rd, Urnes K, Kerwin WS, Bolson EL, Chung T, Kovalchin JP, Sahn DJ, Jerosch-Herold M, Stolpen AH. Three-dimensional shape analysis of right ventricular remodeling in repaired tetralogy of Fallot. *Am J Cardiol* 2008; **101(1)**: 107-13.
 - 17) Bodhey NK, Beerbaum P, Sarikouch S, Kropf S, Lange P, Berger F, Anderson RH, Kuehne T. Functional analysis of the components of the right ventricle in the setting of tetralogy of Fallot. *Circ Cardiovasc Imaging* 2008; **1(2)**: 141-7.
 - 18) Zheng Y, Barbu A, Georgescu B, Scheuering M, Comaniciu D. Four-chamber heart modeling and automatic segmentation for 3-D cardiac CT volumes using marginal space learning and steerable features. *IEEE Trans Med Imaging* 2008; **27(11)**:1668-81.
 - 19) Arun KS, Huang TS, Blostein SD. Least-squares fitting of two 3-d point sets. *IEEE Trans Pattern Anal Mach Intell* 1987; **9(5)**:698-700.
 - 20) Durrleman S, Pennec X, Trouvé A, Ayache N. Statistical models of sets of curves and surfaces based on currents. *Med Image Anal* 2009; **13(5)**: 793-808.

- 21) Vaillant M, Glaunès J. Surface matching via currents. *Inf Process Med Imaging* 2005; **19**:381-92.
- 22) Mansi T, Durrleman S, Bernhardt B, Sermesant M, Delingette H, Voigt I, Lurz P, Taylor AM, Blanc J, Boudjemline Y, Pennec X, Ayache N. A statistical model of right ventricle in tetralogy of Fallot for prediction of remodeling and therapy planning. *Med Image Comput Comput Assist Interv* 2009; **12 (Pt 1)**:214-21.
- 23) Wald RM, Haber I, Wald R, Valente AM, Powell AJ, Geva T. Effects of regional dysfunction and late gadolinium enhancement on global right ventricular function and exercise capacity in patients with repaired tetralogy of Fallot. *Circulation* 2009; **119(10)**:1370-7.
- 24) Kutty S, Zhou J, Gauvreau K, Trincado C, Powell AJ, Geva T. Regional dysfunction of the right ventricular outflow tract reduces the accuracy of Doppler tissue imaging assessment of global right ventricular systolic function in patients with repaired tetralogy of Fallot. *J Am Soc Echocardiogr* 2011; **24(6)**:637-43.
- 25) Bonnemains L, Stos B, Vaugrenard T, Marie PY, Odille F, Boudjemline Y. Echocardiographic right ventricle longitudinal contraction indices cannot predict ejection fraction in post-operative Fallot children. *Eur J Echocardiogr* 2012; **13(3)**:235-42.
- 26) Sarikouch S, Koerperich H, Dubowy KO, Boethig D, Boettler P, Mir TS, Peters B, Kuehne T, Beerbaum P. German Competence Network for Congenital Heart Defects Investigators. Impact of gender and age on cardiovascular function late after repair of tetralogy of Fallot. *Circ. Cardiovasc Imaging* 2011; **4**:703-711.
- 27) Marianeschi SM, Santoro F, Ribera E, Catena E, Vignati G, Ghiselli S, Pedretti S, Suleyman O, Ustunsoy H, Berdat PA. Pulmonary valve implantation with the new Shelhigh Injectable Stented Pulmonic Valve. *Ann Thorac Surg* 2008; **86(5)**:1466-72.

- 28) Guccione P, Milanesi O, Hijazi ZM, Pongiglione G. Transcatheter pulmonary valve implantation in native pulmonary outflow tract using the Edwards SAPIEN™ transcatheter heart valve. *Eur J Cardiothorac Surg* 2012; **41(5)**:1192-4.
- 29) Zhang H, Wahle A, Johnson RK, Scholz TD, Sonka M. 4-D cardiac MR image analysis: left and right ventricular morphology and function. *IEEE Trans Med Imaging* 2010; **29(2)**:350-64.